Title: Functional and optical properties of Au:TiO_2 nanocomposite films: the influence of thermal annealing

Authors: M. Torrell, L. Cunha, A. Cavaleiro, E. Alves, N.P. Barradas, F. Vaz

PII: S0169-4332(10)00555-6
DOI: doi:10.1016/j.apsusc.2010.04.043
Reference: APSUSC 20100

To appear in: *APSUSC*

Received date: 22-2-2010
Revised date: 12-4-2010
Accepted date: 13-4-2010

Please cite this article as: M. Torrell, L. Cunha, A. Cavaleiro, E. Alves, N.P. Barradas, F. Vaz, Functional and optical properties of Au:TiO_2 nanocomposite films: the influence of thermal annealing, *Applied Surface Science* (2008), doi:10.1016/j.apsusc.2010.04.043

Functional and optical properties of Au:TiO_2 nanocomposite films: the influence of thermal annealing

M. Torrell[1*], L. Cunha[1], A. Cavaleiro[2], E. Alves[3], N.P. Barradas[3], F. Vaz[1]

[1]Universidade do Minho, Dept. Física, Campus de Azurém, 4800-058 Guimarães, Portugal
[2]SEC-CEMUC – Universidade de Coimbra, Dept. Eng. Mecânica, Pólo II, 3030-788 Coimbra, Portugal
[3]Instituto Tecnológico e Nuclear, Dept. Física, Apartado 21, E.N. 10, 2686-953 Sacavém, Portugal

*E-mail: marc.faro@fisica.uminho.pt

Abstract
A set of nanocomposite thin films consisting of Au nanoclusters dispersed in a TiO_2 dielectric matrix were deposited by reactive magnetron sputtering, and subjected to thermal annealing in vacuum, at temperatures ranging from 200 to 800 ºC. The obtained results show that the structure and the size of Au clusters, together with the matrix crystallinity, changed as a result of the annealing, and were shown to be able to change the optical properties of the films and keeping good mechanical properties, opening thus a wide number of possible applications. The crystallization of the gold nanoclusters induced by the annealing was followed by a systematic change in the overall coating behaviour, namely the appearance of Surface Plasmon Resonance (SPR) behaviour. This effect enables to tailor the thin films reflectivity, absorbance and colour coordinates, contributing for the importance of this thin film system. The different attained optical characteristics (reflectance values ranging from interference to metallic-like behaviours and colour varying for interference rainbow-like to several tones of red brownish), associated with a reasonable mechanical resistance of the coatings (good adhesion to different substrates and hardness values ranging from 5-7.5 GPa), induce the possibility to use this film system in a wide range of decorative applications.

Keywords: Decorative thin films, Gold, Surface Plasmon Resonance, TiO_2, mechanical properties

1. Introduction

Decorative surface treatments of consumer goods have a high interest, because of their wide possibility for application in different industrial branches. In this domain, vacuum-based methods (PVD, plasma-CVD, etc.) have established themselves in the actual market as important competitors to lacquering and electrochemical classic processes [1,2]. In a general way, at the surface of decorative objects, two different

physical processes can be responsible for the appearance of a particular surface tone aspect: interference and intrinsic colours, which are generated via selective phenomena of absorption and reflection of light [2]. An intrinsic colour can be reached, among others, by the activity of the so-called Surface Plasmon Resonance (SPR) phenomena on nanocomposite thin films [3], as it is the example of metallic nanoparticles dispersed in dielectric amorphous mediums [4]. An important feature that contributes for the variation of the SPR effect is the change in the inter-grain distances of the metallic particles dispersed in the dielectric medium, by changing their matrix population. Furthermore, a wide range of chemical-physical properties can also be reached in these nanocomposites films by varying the morphology of these particles [5,6]. Among the most common features, one can include the size, distribution and shape of the nanoparticles. A strong local field effect arises from the dielectric confinement and shows a maximum at the so-called SPR frequency where the quantized collective motion of the confined free electrons is resonantly-coupled to the incident optical field, yielding characteristic absorption bands [6]. However, only metals with free electrons (e.g. Au, Ag and Cu) possess Plasmon Resonances in the visible spectrum, which can give rise to intense and attractive colourations [7]. It is known that these metals offer a quasi-free-electron behaviour on the UV-visible range. Gold nanoparticles (GNPs) are commonly selected as a cluster to reach the SPR effect on TiO_2 dielectric matrixes, as it is the case in the present work.

As already mentioned, the optical properties of these nanocomposite-like films have a critical dependence on the GNPs microstructure, size, shape and volume factor, but also on the dielectric properties of the host matrix itself [8-10]. This dependence can be used in a wide range of high technological applications, including the decorative

field (gold particles provide different colours in roman glasses and medieval cathedrals windows for centuries), but also as colour filters [11], bio and optical sensors [3,12,13] absorption elements of solar cells [12], electrical/thermal conductivity [12], antibacterial [14], etc. Anyway, most of these sensor applications rely on colloidal solutions, which may represent restrictions for some applications, and thus opening some widows of opportunity for the thin film-based technologies, such as the one mentioned in the present work: reactive magnetron sputtering.

The preparation of materials where metallic nanoparticles are dispersed in non-aqueous dielectric media (latex, polystyrene, TiO_2, SiO_2, etc…), using for example PVD (where the specific technique used in this work is included) or CVD technologies, is actually becoming one of the most important fields in specific areas of materials science, integrating a new aim for the use of nanoscience and nanotechnology [3,14,15]. When nanocomposite thin films, such as those of Au dispersed nanoclusters in dielectric TiO_2, Au:TiO_2, are deposited by sputtering, the changes of the deposition parameters and post-deposition annealing treatments, can offer some possibilities to change all, or part, of the key factors influencing the optical behaviour, and thus improving their competitiveness in relation to the electrochemical baths, due to be a non-polluting technique. The great advantage will be to allow overcoming the restrictive normatives that are being applied on the decorative and protector electrochemical films industry.

Nevertheless, the use of such nanocomposite films needs a fundamental understanding of their properties if their suitability for a particular purpose is to be envisaged. There is a general agreement in literature that the performance of coated devices and components in any real application is mainly determined by the properties of near-surface layers [16]. This implies that the solutions to achieve a coating tailored

for a particular application in the decorative field will essentially depend on the ability to achieve a suitable performance concerning optical as well as mechanical properties. In order to maintain or increase the lifetime of a particular decorative coated object/device, hardness as well as the coating adhesion levels have been extensively adopted as fundamental properties for quality and process control.

Taking all the above into account, the main goal of the present work was thus to prepare Au:TiO_2 nanocomposites coatings and to study their optical behaviour as a function of the structural features that resulted from different annealing temperatures. Taking into account the possibility to use such nancomposites in some of the already mentioned applications, a detailed study of their functional properties will also be carried out and correlated with the structural features.

2. Experimental Procedure

A batch of Au:TiO_2 thin films was deposited onto silicon (100) and quartz substrates by dc reactive magnetron sputtering, in a laboratory-sized deposition apparatus. Two vertically opposed rectangular magnetrons (unbalanced of type 2) were disposed in a closed field configuration in the deposition chamber. Only one electrode was powered, composed of a titanium target (99.6 % purity), with 8 Au pellets (with a 40 mm^2 surface area and approximately 2 mm thickness), symmetrically incrusted in its preferential eroded zone. A constant dc current density of 100 A m^{-2} was applied. A mixture of argon and oxygen was injected with constant fluxes of 60 sccm and 10 sccm, corresponding to partial pressures of 0.3 Pa and 0.08 Pa, respectively. The final working pressure (~0.38 Pa) was kept approximately constant during the entire coating deposition process. The deposition temperature was close to 200 °C [17]. Samples were

placed in a rotating substrate holder (7 rpm) in grounded condition. All samples were heat treated through annealing experiments, in vacuum, after film deposition. Annealing treatments were carried out in a secondary vacuum furnace, after its evacuation to about 10^{-4} Pa. The selected temperature range varied from 200 to 800 °C, and the isothermal period was fixed to 60 min, after a heating ramp of 5 °C/min. The samples cooled down freely in vacuum before their removal to room conditions. Chemical composition of the coatings was investigated with a Cameca SX-50 Electron Probe Micro Analysis (EPMA), operating at 15 keV. The elemental quantification was performed by comparing the peak intensity in the sample with standards for each element, and applying a ZAF correction to the results. The chemical uniformity of the films throughout their entire thickness was check by Rutherford backscattering spectrometry (RBS), carried out in a IBA Data Furnace NDF v9.2e at 2 MeV with He^{++} with an scattering angles of 140° (standard detector) and 180° (annular detector) and incidence angles of 0 and 20° [18]. All coatings were characterized by X-ray diffraction (XRD), using a Philips PW 1710 diffractometer (Cu-Kα radiation), operating in a Bragg-Brentano configuration. XRD patterns were deconvoluted, assuming to be Voigt functions to yield the peak position, integrated intensity and integrated width (IntW). These parameters allow calculating the interplanar distance, preferential orientation and grain size.

Optical properties (Transmittance-absorbance) were characterized using a UV–Vis–NIR Spectrophotometer (Shimadzu UV 3101 PC) in the spectral range from 200 nm to 900 nm. SEM images of the coatings have been obtained by a NanoSEM FEI Nova 200 scanning microscopy. Scratch tests were performed with constant loads, between 2 and 80 N, and at a fixed load rate of 1.5 N/s, and a scratching track of 0.01 m, using a

Revetest Scratch tester (CSM Instruments). The visual study of the scratch has been done using 100 and 500 magnifications in the optical microscopy [19]. Nanoindentation on the films was performed on a MicroMaterials apparatus, equipped with a diamond Berkovich indenter. Hardness and elastic modulus were determined from the load versus depth data. The peak load used was 0.8 mN. The values reported here were averaged ones from 2 series of 15 indentations carried out in two different zones of the coated sample.

3. Results and discussion

3.1 Composition and structure

The Au concentration in the samples, studied by EPMA, was found to be close to 12 at. %. The elemental concentration analysis also revealed that the ratio O/Ti was always very close to 2, which suggests the presence of a stoichiometric-like TiO_2 matrix, with no apparent variation during the annealing experiments (as far as it concerns the resolution of the measurement techniques). The Au content in all films has been selected based on previous published results, where it was reported that the range between 10 and 20 at. % Au conducted to the clearest SPR activity on the optical properties [15]. Thickness measurements carried out by SEM observation (cross-section view, Fig. 1) showed that the films have approximately 300 nm. Au volume fraction, f_{Au}, was determined as being close to 0.18 (considering $\rho(Au) = 19.3$ g/cm^3 and $\rho(TiO_2) = 4$ g/cm^3).

The cross-section morphology of the films, studied by SEM, is shown on Fig. 1. From the observation of this micrograph, it is clear that the film grows in a compact and dense featureless structure, without any special characteristics - featureless growth.

Important to note also is that, in spite of the small round features observed in SEM micrographs, the use of backscattering electron images undoubtedly showed that no Au agglomerations signs were detected, at least within the 2 nm maximum lateral resolution of the used SEM instrument. Very similar results were also observed in the annealed samples, which gave no conclusive results about the morphological variations that may occurred as a result of the annealing process. In order to check for clear evidences of any (micro)structural changes, which could then be used to correlate with the overall coatings behaviour, an extensive set of XRD experiments were carried out. The diffraction profiles have been studied in the as-deposited and in the annealed samples. Figure 2 shows the obtained results as a function of the annealing temperature. From this set of results, it can be clearly stated that the as-deposited films show an amorphous-type structure, without any visible traces of crystalline Au or any of the known crystalline phases of titanium oxides. However, the annealing process lead to the crystallization of the amorphous films, firstly by the detection of crystalline Au, followed by some crystallization of the TiO_2 matrix, but with this last occurring only for temperatures above 400 ºC (T > 400 °C). The presence of Au, with a fcc-like structure [ICDD card Nº 04-0787], is evidenced for annealing temperatures above 200 °C, as it can be observed by the presence of the (111) peak, localized at $2\theta = 38.2°$, as well as the (200) peak, at $2\theta = 44.4°$, with this last one appearing for annealing temperatures above 400 ºC, exactly at the temperature where the first signs of TiO_2 crystallization have also appeared.

Furthermore, a careful observation of the XRD patterns shows also that the initial broad Au (111) peak, which starts to be detected at an annealing temperature of 300 °C, becomes sharper with the annealing treatments, as a result of the grain growth, probably

due to the coalition of Au atoms. The Au clusters grow in size as the annealing temperature increase, which is followed by some crystallization of the remaining amorphous oxide dielectric matrix that occurs at an annealing temperature around 500 ºC. The diffraction patterns seem to indicate that this amorphous TiO_2 matrix crystallizes in the anatase form [ICDD 21-1272], as in fact suggested in similar studies where annealing of TiO_2-based films is involved [20]. These results suggest that, at this temperature, a nanocomposite film consisting of a crystalline dielectric TiO_2 matrix embedded with Au clusters was formed. At annealing temperatures above 700° C, the TiO_2 phase changes from the anatase to the rutile [ICDD 21-1276] structure, which is in accordance with results available in the literature [21,22]. The access of this nanocomposite structure up to 500 ºC should be responsible for the appearance of SPR activity, which can be used to tune some of the film properties, namely the optical ones, as it will be shown later on in this text. On the other hand, it is not entirely clear the role of the structural transformations of the dielectric matrix, TiO_2, from amorphous to crystalline and from anatase to rutile, which was detected between 500 and 800 °C. Anyway, the overall set of results that were obtained in the frame of the present work seems to indicate that the structural changes indexed to the Au clusters may be more important for the SPR activity. As it is further detailed on the following sections, the first evidences of the Au crystallization (300 ºC) are found to correspond also to the main changes on the optical properties (reflectivity, colour and absorbance).

In terms of results summary, this first set of data indicates that the samples can be arranged in three different groups, which will have also a correspondence in the optical and colour measurements, as it will be discussed on following sections. The first two of samples (as-deposited and 200 ºC annealed samples) show no evidences of any

crystalline Au (samples group I), while the samples annealed at temperatures of 300 and 400 ºC show some clear signs of gold crystallization, revealing though very broad peaks, a sign of very small clustering sizes (samples group II). This second group could be defined as an intermediate step towards a third group of samples (group III), where the higher annealing temperature induced more crystalline samples, together with a clear reduction on the with of the Au diffraction peaks at half maximum (FWHM), which is a sign of the continuous growth of the Au clusters (coalescence), and also some traces of the oxide matrix crystallization. These features will have an important role in the SPR activity, as shown latter in the text.

Fig. 3 shows the results of the average size (diameter) of the gold particles in the nanocomposite films, based on the integral-breadth analysis of the XRD patterns. The values of gold particles (clusters) size range from about 2 nm at 300 °C to approximately 13 nm at 700 °C. In accordance of the results plotted in Fig. 3, the Au particles are confined on the nanometrical scale, with its growth lead by the diffusion of the Au atoms promoted by the thermal energy (annealing). The SPR activity and the related changes on the optical properties are directly affected by this growth. Fig. 3 clearly illustrates the increasing on the Au particles size is continuous in this range of temperatures. The main SPR activity has been reported between 400 °C – 600 °C, where the average grain size is within 3 nm to 10 nm [13]. At temperatures below 300 °C no important SPR activity has been found, where the size of Au clusters are too small to be considered as a phase crystal structure dispersed on the dielectric matrix.

3.2 Optical properties

The influence of the Au clusters size embedded within the dielectric matrix on the SPR activity was accessed by reflectivity, absorbance and colour measurements. Different reflectivity behaviours were found in the annealed samples, when compared to the as-deposited ones. The interferometric behaviour disappears at 300 ºC as can be observed in Fig. 4, and corresponding in fact to the change from the set of samples group I to those from group II, as stated in the previous section. The reflectance spectra shows a clear change from interference-like (interference bands are clearly visible for the as-deposited and 200 ºC annealed samples, samples from group I) to an intrinsic behaviour similar to the one obtained for pure Au [14] (intrinsic metallic-like optical behaviour), with the increase of the annealing temperature. The samples annealed at temperatures above 200 ºC (groups II and III) show a minimum of reflection close to 500 nm, followed by a progressive increase of the reflection intensity in the highest wavelength of the visible region of the electromagnetic spectrum. The minimum is reached at quite similar values of the wavelength (500-515nm) with a slight blue shift with increasing annealing temperatures. Furthermore, with this temperature variation, there is a clear tendency for having positive slope of the reflection steeper for wavelengths higher than the minimum of the reflectance (transition from samples of group II to those of group III).

As stated above, there is a straight correlation between these changes and the XRD results. In fact, the disappearance of the interferometric features in the reflectance spectra occurs at the same annealing temperature where the Au crystallization starts to be detected (change for the set of samples indexed to group II), promoted by Au clusters coalescence, which seems to confirm the major role of gold morphological and structural changes in the films behaviour. In these conditions, Au is most probably

dispersed in the TiO_2 amorphous dielectric matrix in the form of individual or very small groups of atoms, which are still not able to form coherent crystals, with the consequent XRD amorphous character and a typically interference-like dielectric matrix. The relatively low values of the reflectivity at shorter wavelengths are characteristic of high free electron density systems [23].

As the annealing temperature increased, $T \geq 300$ °C (film zones II and III), the behaviour of the films changed from interference-like to intrinsic-like, as revealed by the film's surface tones that tend rapidly to a red-brownish colour, in comparison to the interferometric tones of the as-deposited and 200 ºC annealed samples (zone I), Fig. 5. As evidenced in Fig. 2, associated with the first change on the reflectivity trend, a broad peak positioned at $2\theta \approx 38°$ was detected in the XRD pattern, which was indexed as Au (111) planes. At higher temperatures, the Au (111) XRD peaks become narrower and more intense, indicating higher crystal sizes (Fig. 3), which is followed by the increase of the reflectivity and the complete vanishing of the interference bands (Fig. 4).

A more detailed analysis of the changes in colour with the thermal treatment was accessed by studying the CIELab colour analysis. As shown in Fig. 5, the change from the interference tones towards the intrinsic red-brownish, is followed by a significant increase of the a* parameter (redness) and a slightly increase of b* parameter (yellowness) of the CIELab scale. The most abrupt change in the a* parameter is detected in the 300 °C annealed sample, again coincident with the Au precipitation and the transition from interference to intrinsic behaviour shown in the reflectivity curves (transition to samples from zone II). It can be stated that the larger is the change on the colour parameters, the larger the change on the reflectivity values reported on Fig. 4.

In order to enhance the Surface Plasmon Resonance (SPR) activity, which should be related with the optical changes above described, absorbance measurements (A = log 1/T) were also carried out in the overall set of samples. SPR is manifested as a distinct peak in the absorbance spectrum [4], and has been reported in several nanocomposite materials through the localization of an absorbance band on the visible wavelength range [4,8,11,20,25,26]. Figure 6 shows the absorbance behaviour of the analysed films. As it would be expected from the complementarities between reflectance, absorbance and transmittance, the differences in the intensity observed on the reflectivity curves are in good agreement with the absorbance curves. Globally, at the same wavelength, higher reflectivity is linked to lower absorbance intensity. The changes in the absorbance spectra can be detected already at 300 ºC, also confirming the first crystallization evidences through the Au clusters precipitation. Important to emphasise is that the SPR activity starts to develop for temperatures above 200 ºC and becomes higher at higher temperatures. At temperatures above 500 ºC, the transmittance of the sample is close to 0 for a wide range of wavelength values, so the absorbance cannot be measured accurately. When the samples were annealed between 300 and 500 ºC, the optical density increases, together with a slightly red shift, already enhanced in the reflectivity measurements. The absorbance peak is shifted from 587 nm to 610 nm. The peak red shift of the Au:TiO_2 samples has to be ascribed to two factors, first the grow of the nanoparticles and the variance in the dielectric constant of titanium oxide matrix that exist as different ratios of amorphous/anatase phases due to the different annealing treatments [4,27]. So the matrix presents a different dielectric constant for each annealing temperature modifying the energy of the SPR absorption, located at larger wavelengths for more crystalline matrixes (higher annealing temperatures).

In general, the absorption peaks are relatively broad, especially those of samples annealed at low temperatures. It is well known that SPR activity depends strongly upon the nanoparticles morphology, namely the size and shape of the metal clusters [4,10]. Thus, peaks broadening may be due to the poor crystallization of the Au clusters and, especially, to the non-uniform clusters shape and distribution. A wide distribution of clusters sizes, which become narrower at higher annealing temperatures, should give rise, as often referred to in the available literature, to the wideness of the absorption peak [20].

From the overall analysis, it is clear that the same different groups of samples that were indexed on the structural discussion are also present on the optical behaviour study. In fact, the optical properties results show that the same three groups can also be claimed. The first group (as-deposited and 200 °C annealed sample) shows that the samples reveal interference-like behaviour (both in reflectance and absorvance), with a surface tone characteristic of interference coloured materials (rainbow-like aspect). The samples from the transition zone (zone II: 300 and 400 ºC annealed samples) show low absorbance results and the colour tones change clearly to intrinsic-like ones, which can be characterized as light red brownish. Finally, there is a group of samples with higher SPR behaviour (samples annealed at 500, 600 and 700 °C), where there is a clear tendency for the darkening of the surface colour tones. This higher effect of the SPR on the samples annealed at temperatures of 500º C or higher, can be clearly seen on the reflectance (Fig. 4), colour coordinates (Fig. 5) and absorbance (Fig. 6) results. It is important to highlight that TiO_2 films do not show any of these optical changes under the same heat treatment [24].

3.3 Functional properties

Whenever a decorative application is envisaged, the mechanical properties should also be taken into account. In fact, the coatings have to resist to everyday use and thus hardness and adhesion to the coated objects should play a fundamental role in improving the lifetime. In the present case, these two properties were checked and their variations studied as a function of the annealing temperatures.

Table I shows the hardness (H) and elastic modulus (E) values of the as deposited and annealed films obtained from the nanoindentation tests. The maximum indentation depths displayed in the table does not allow to accomplish the largely used rule of the 1/10 in coated samples (the ratio between the indentation depth and the film thickness should be lower than 1/10 - Buckle law, see e.g. [31]). However, this rule is far apart from reality when the ratio between the hardness of the coating and substrate is considered (H_f/H_s). The ratio between critical indentation depth (hc) and film thickness (t) is much lower than 1/7 when the H_f/H_s ratio is equal or lower than 1 [32-35]. The H_f/H_s ratio between Au:TiO_2 deposited films and Si (100) approaches values of 0.6, thus leading to critical hc/t ratios which should be expected to be close from 1/4 to 1/6. Taking into account the maximum penetration depth (in the range from 45 to 60 nm) and the film thickness close to 300 nm, no great influence of the substrate is expected in the H measurements. Nevertheless, as H results in table 3 are taken in the same coating with increasing temperatures, the trends which can be extracted from the table analysis should not be influenced by any possible substrate influence in the measured values.

Two clear inverse trends could be identified for the hardness with the temperature increase, the first up to 400 ºC, decreasing, and the second, increasing, for higher annealing temperatures. The evolution of the hardness can be interpreted as a function

of two main factors, the residual stresses and the Ti-O matrix crystallization. With the conditions used for depositing the coatings (low discharge pressures) sputtered films are usually under compression mainly due to the energetic neutrals bombardment during film growth [28]. During annealing, the compressive residual stresses can decrease and even change their sign for tensile. Firstly, the Au clusters precipitation will promote a decrease of the global specific volume by the atomic arrangement during Au clusters formation. Secondly, during the annealing stress relaxation is expected. During cooling down to room temperature, "new" stresses will be generated resulting from the difference in the thermal expansion coefficient between the coating (α_f) and the substrate (α_s). These stresses should be of tensile type since the α_{TiO2} ($8\text{-}12.10^{-6}$ $K\text{-}^{-1}$) is higher than α_{Si} ($2\text{-}4.10^{-6}$ K^{-1}) [29]. Thus, with increasing annealing temperature a tensile stress component is being introduced in the coatings leading to a decrease in their hardness values, as it is well known in the literature [30].

For temperatures higher than 500 ºC, the crystallization of the Ti-O matrix takes place and the coatings become more and more crystalline, although keeping a nanometric level. The crystallization is usually associated to an improvement of the mechanical properties of sputtered coatings [28,29]. This phenomenon will counterbalance the softening induced by the tensile residual stress component leading to a net increase of the hardness for the highest annealing temperatures studied. Similar trend has been observed for the reduced Young´s modulus, a behaviour which is usually connected to an increase in brittleness for a material. [36,37].

Generally, the hardness of sputtered Au:TiO_2 thin films is higher than that of similar coatings produced by other methods as sol-gel [38]. However, the nanocomposite films, by PVD or CVD, show in all the cases, values much lower than

the 13.4 GPa reported for the pure TiO_2 tested under similar conditions [39]. The presence of the metal clusters, more ductile relatively to the ceramic matrix of the film, should be responsible for the initial drop of nanohardness [40].

Regarding the scratch testing behaviour, table I summarizes the evolution of the critical load values, when the scratch test was performed on the glass coated samples. The classical critical loads, Lc_1, Lc_2 and Lc_3, are defined respectively as the first crack (corresponding to cohesive failures), first interfacial (adhesive) failure, and finally massive interfacial failure (shell shaped failure in the studied samples). In the case of this work, only L_i and L_f were defined corresponding to the first cohesive failure event and the adhesive failure, respectively. The samples show Lc_2 and Lc_3 very close without any appreciable variation between them, motivating the use of a unique adhesive value, L_f. As it is described on the standards of the scratch test [**Error! Bookmark not defined.**], a reward cracking morphology was found typical from low values of adhesion, the curve of the cracks showing the convex part on the backside of the indenter. This crack morphology (Fig. 7a) and 7b) is defined as Hertzian type circular cracks and the mechanisms of formation are lead for a successive compressive-tensile cyclic state of the film during the test.

Keeping the same mechanisms on all the studied samples, an important decreasing of the L_f value is shown after annealing, with the decohesion from the substrate occurring at lower loads. No signs of ductile deformation are visible confirming the brittle behaviour of the films. The presence of the tensile component of the stress in the annealed films should contribute for their easier flaking from the substrate as confirmed by the lower values of the Lc_f critical load.

4. Conclusions

After the study of the influence of the annealing temperature on the Au:TiO_2 sputtered film on their structure, and optical and functional properties, it can be conclude that: Structural conditions to reach SPR are achieved for annealed samples above 300 °C, which is clearly shown on the optical properties and colour measurements. The main factor for the presence of SPR seems to be the growth of gold nanoparticles and their redistribution in the dielectric matrix. Other factors as TiO_2 phase or crystalline matrix ratio seems to play a secondary role, shifting the position of the SPR bands at higher wavelengths. All the changes on the optical properties are consistent with the changes on crystal grain size studied on the XRD profiles. Since annealing treatments are carried out slight variations of the nanohardness and reduced Young modulus are reported because of the redistribution of the residual stresses combined with the crystallization of the matrix and Au metallic particles. This matrix crystallization leads to the net increase of both parameters (H_B and E) for the highest annealing treatments studied. The brittle behaviour of the crystallized ceramic matrix and the presence of the tensile components on the residual stresses lead to the drop on the Lc_f. The adhesion of the film keeps good values even at higher annealed temperatures. It can be conclude that sputtered Au:TiO_2 thin films can be appropriate for decorative applications due to their optical and functional properties.

5. Acknowledgments

The authors acknowledge the Portuguese Science Foundation "Fundação para a Ciência e Tecnologia - FCT" for the project PTDC/CTM/70037/2006.

6. References

[1] B. Navinsek, P. Panjan, I. Milosev, PVD coatings as an environmentally clean alternative to electroplating and electroless processes, Surf. Coat. Technol. 116–119 (1999) 476–487.

[2] M. Fenker, N. Jackson, M. Spolding, P. Nicole, K. Schönhute, G. Gregory, P.E. Hovsepian, W.D. Munz, Corrosion performance of PVD-coated and anodised materials for the decorative market, Surf. Coat. Technol. 188–189 (2004) 466– 472.

[3] E. Hutter, J.H. Fendler, Exploitation of Localized Surface Plasmon Resonance, Adv. Mater. 16(19) (2004) 1685-1706.

[4] M. Lee, L. Chae, K.C. Lee, Microstructure and surface plasmon absorption of sol-gel-prepared Au nanocluster in TiO_2 thin film, Nanostruct. Mater. 11(2) (1999) 195-201.

[5] S.K. Mandal, R.K. Roy, A K. Pal, Surface plasmon resonance in nanocrystalline silver particles embedded in SiO_2 matrix, J. Phys. D: Appl. Phys. 35(17) (2002) 2198-2205.

[6] S.H. Cho, S. Lee, D. Y. Ku, T. S. Lee, B. Cheong, W.M. Kim, K.S. Lee, Growth behavior and optical properties of metal-nanoparticle dispersed dielectric thin films formed by alternating sputtering, Thin solid films 447-448 (2004) 68-73.

[7] L.M. Liz-Marzán, Nanometals: Formation and Color, Mater. Today 7(2) (2004) 26-31.

[8] D. Dalacu, L. Martinu, Spectroellipsometric characterization of plasma-deposited Au/fluoropolymer nanocomposite films, J. Vac. Sci. Technol. A 17(3) (1999) 877-883.

[9] S. Cho, S. Lee, S. Oh ,S.J. Park, W.M. Kim, B. Cheong, M. Chung, K.B. Song, T. S. Lee, S.G. Kim, Optical properties of Au nanocluster embedded dielectric films, Thin solid films 377-378 (2000) 97-102.

[10] D. Dalacu, L. Martinu, Spectroellipsometric characterization of plasma-deposited Au/SiO_2 nanocomposite films, J. Appl. Phys 87(1) (2000) 228-235.

[11] H. Takele, H. Greve, C. Pochstein, V. Zaporojtchenko, F. Faupel, Plasmonic properties of Ag nanoclusters in various polymer matrices, Nanotechnology 17 (2006) 3499-3505.

[12] G. Walters, I. P. Parkin, The incorporation of noble metal nanoparticles into host matrix thin films: synthesis, characterisation and applications, J. Mater. Chem. 19(5) (2009) 574-590.

[13] M. Torrell, P. Machado, L. Cunha, N.M. Figueiredo, J.C. Oliveira, C. Louro, F. Vaz, Development of new decorative coatings based on gold nanoparticles dispersed in an amorphous TiO_2 dielectric matrix, Surf. Coat. Technol. 204 (2010) 1569–1575.

[14] C.M. Wang, V. Shutthanandan, Y. Zhang, S. Thevuthasan, L. E. Thomas, W. J. Weber, G. Duscher, Atomic level imaging of Au nanocluster dispersed in TiO_2 and $SrTiO_3$, Nucl. Instrum. Methods Phys. Res. Sect. B 242 (2006) 448-450.

[15] L. Armelao, D. Barreca, G. Bottaro, A. Gasparotto, S. Gross, C. Maragno, E. Tondello, Recent trends on nanocomposites based on Cu, Ag and Au clusters: A closer look, Coord. Chem. Rev. 250 (11-12) (2006) 1294-1314.

[16] Y. Pauleu, P.B. Barna, "Protective Coatings and Thin Films, Synthesis, Characterization and Applications (nato Science Partnership Sub-series: 3: High Technology, Volume 21 ed., Y. Pauleau and P.B. Barna, Kluwert Academic publishers, Dodrecht, Netherlands, 1997.

[17] P. Carvalho, J.M. Chappé, L. Cunha, S. Lanceros-Méndez, P. Alpuim, F. Vaz, E. Alves, C. Rousselot, J.P. Espinós, A. R. González-Elipe, Influence of the chemical and electronic structure on the electrical behavior of zirconium oxinitride films, J Appl. Phys. 103 (2008) 104907-104915.

[18] N.P. Barradas, C. Jeynes, R.P. Webb, Simulated annealing analysis of Rutherford backscattering data , Appl. Phys. Lett. 71 (1997) 291-293.

[19] EUROPEAN STANDARD. EN 1071-3, EN1071-3: Advanced technical ceramics. Methods of test for ceramic coatings. Determination of adhesion and other mechanical failure modes by scratch test.

[20] M.G. Manera, J. Spadavecchia, D. Buso, C. de Julian-Fernandez, G. Mattei, A. Martucci, P. Mulvaney, J. Pérez-Juste, R. Rella, L. Vasanelli, P. Mazzoldi, Thin films of TiO_2 nanocrystals with controlled shape and surface coating for surface plasmon resonance alcohol vapour sensing, Sens. Actuators, B 132(1) (2008) 107-115.

[21] M. Hasan, A. Haseeb, R. Saidur, H. Masjuki, M. Hamdi, Influence of substrate and annealing temperatures on optical properties of RF-sputtered TiO_2 thin films, Opt. Mater. (2009) In Press. doi:10.1016/j.optmat.2009.07.011.

[22] N. Martin, C. Rousselot, D. Rondot, F. Palmino, R. Mercier, Microstructure modification of amorphous titanium oxide thin films during annealing treatment, Thin solid films 300 (1-2) (1997) 113-121.

[23] L. Yate, L. Martínez-de-Olcoz, J. Esteve, A. Lousa, Control of the bias voltage in d.c. PVD processes on insulator substrates, Vacuum 83(10) (2009) 1287-1290.

[24] A. Dakka, J. Lafait, M. Abd-Lefdil, C. Sella, M. Maaza, Optical study of Ag-TiO2 nanocermet thin films prepared by R.F. co-sputtering Eur. Phys. J. Appl. Phys 9 (2000) 105-114.

[25] K. Zakrzewska, M. Radecka, A. Kruk, W. Osuch, Noble metal/titanium dioxide nanocermets for photoelectrochemical applications, Solid State Ionic 157(1-4) (2003) 349-56.

[26] J. Vosburgh, R.H. Doremus, Optical absorption spectra of gold nano-clusters in potassium borosilicate glass, J. Non-Cryst. Solids 349 (2004) 309-314.

[27] J. Wang, W.M. Lau, Q. Li, Effects of particle size and spacing on the optical properties of gold nanocrystals in alumina, J. Appl. Phys. 97 (11) (2005) 114303-114308.

[28] K.R. Wu, C.H. Ting, J.J. Wang, W.C. Liu, C.H. Lin, Characteristics of graded TiO_2 and TiO_2/ITO films prepared by twin DC magnetron sputtering technique, Surf. Coat. Technol. 200 (20-21) (2006) 6030-6036.

[29] CES EduPack – CES Selector version 5.1.0, Copyright Granta Design Limited.

[30] A. Cavaleiro, A.P. Marques, J.V. Fernandes, N.J.M. Carvalho, J.Th. De Hosson, Evolution of the microstructure, residual stresses, and mechanical properties of W-Si-N coatings after thermal annealing, J. Mater. Res. 20 (2005) 1356-1368.

[31] G. Berg, P. Grau, Influence of the Substrate Hardness on the Validity of Bückle's Rule, Crys. Res. and Tech. 28 (2006) 989-994.

[32] I. Manika, J. Maniks, Effect of substrate hardness and film structure on indentation depth criteria for film hardness testing. J. Phys. D: Appl. Phys. 41 (2008) 740101 -740106.

[33] I. Manika , J. Maniks, Characteristics of deformation localization and limits to the microhardness testing of amorphous and polycrystalline coatings Thin Solid Films 208 (1992) 223-227.

[34] D. Lebovier, P. Gilormini, E. Felder, A kinematic model for plastic indentation of a bilayer Thin Solid Films 172 (1989) 227-239.

[35] N. Panich, Y. Sun Y, Effect of penetration depth on indentation response of soft coatings on hard substrates: a finite element analysis, Surf. Coat. Technol. 182 (2004) 342-350.

[36] A.C. Fernandes, F. Vaz, L. Cunha, N.M.G. Parreira, A.Cavaleiro, Ph. Goudeau, E. Le Bourhis, J.P. Rivière, D. Munteanu, B. Borcea, R. Cozma, The influence of structure changes in the properties of TiC_xO_y decorative thin films, Thin solid films 515 (13) (2007) 5424-5429.

[37] S. Carvalho, E. Ribeiro, L. Rebouta, C. Tavares, J.P. Mendonta, A. Caetano Monteiro, Microstructure, mechanical properties and cutting performance of superhard (Ti,Si,Al)N nanocomposite films grown by d.c. reactive magnetron sputtering, Surf. Coat. Technol. 177-178 (2004) 459-468.

[38] W. Liu, Y.Chen, G.T. Kou, T. Xu, D.C. Sun, Characterization and mechanical/tribological properties of nano Au-TiO_2 composite thin films prepared by a sol-gel process, Wear 254 (10) (2003) 994-1000.

[39] A.R. Bally, P. Hones, R. Sanjine, P.E. Schmid, F. Levy, Mechanical and electrical properties of fcc TiO_{1+x} thin films prepared by r.f. reactive sputtering, Surf. Coat. Technol. 108–109 (1998) 166–170.

[40] O. Anderson, C.R. Ottermann, R. Kuschnereit, P. Hess, K. Bange Fresenius, Density and Young modulus of thin TiO_2 films, J. Anal. Chem. 358 (1) (1997) 315-318.

Figure captions

Fig. 1. SEM-SE micrograph of the film cross section.

Fig. 2. XRD difractograms of Au:TiO_2 sample series as a function of the annealing temperature.

Fig. 3. Grain size obtained by integral-breadth analysis of Au:TiO_2 at different annealing temperatures.

Fig. 4. Reflectivity as a function of the annealing temperature of Au:TiO_2 samples.

Fig. 5. CIELa*b* variation with the annealing temperature of Au:TiO_2 samples.

Fig. 6. Absorbance Spectra of Au:TiO_2 at different annealing temperatures

Fig. 7. a) Morphology of hertzian cracks during the track of scratch test; **b)** Final step of the scratch test where it can be seen that the whole film is spalled at L_f.

Fig. 1. SEM-SE micrograph of the film cross section.

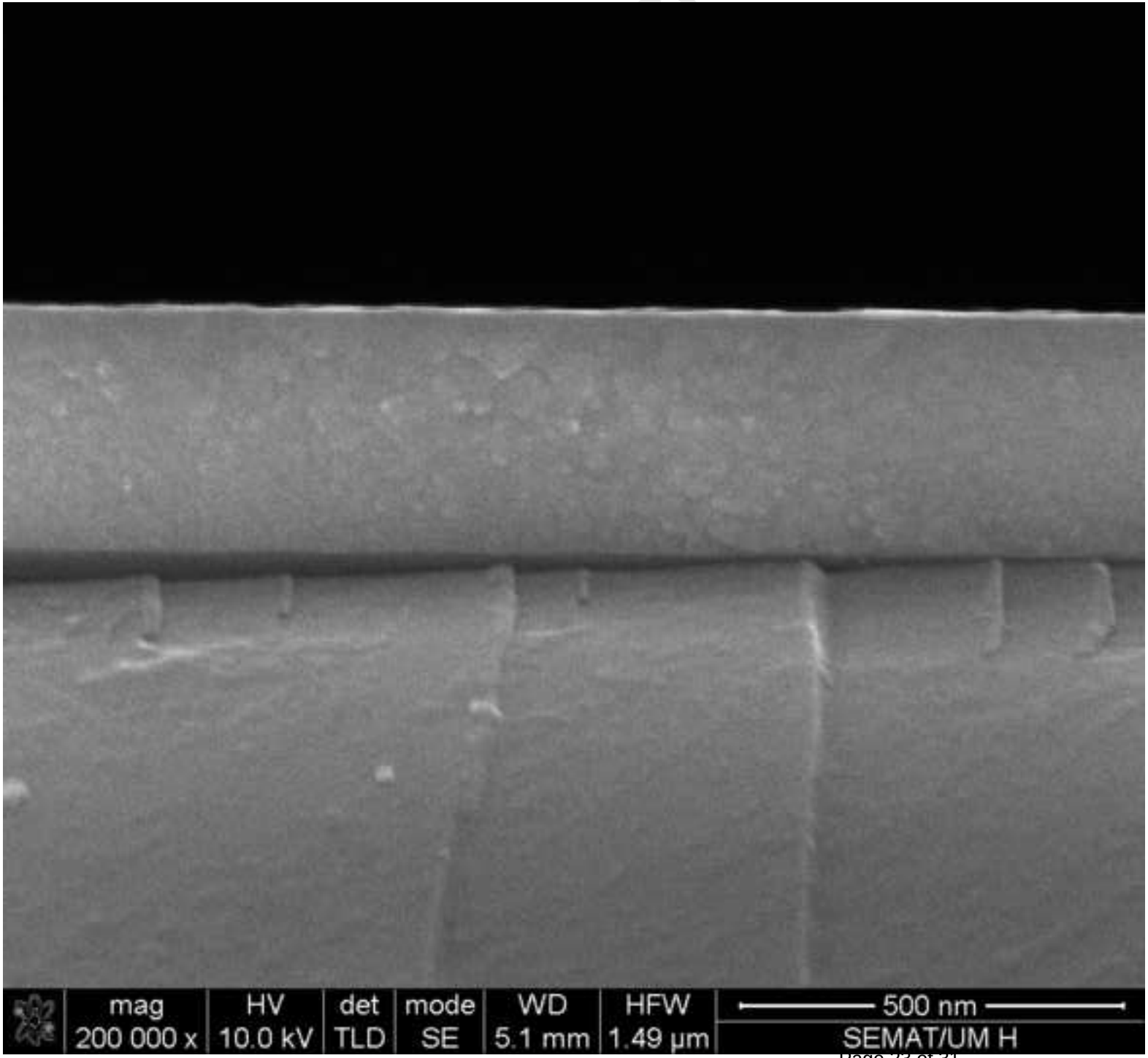

Fig. 2. XRD difractograms of Ti:O-Au sample series as a function

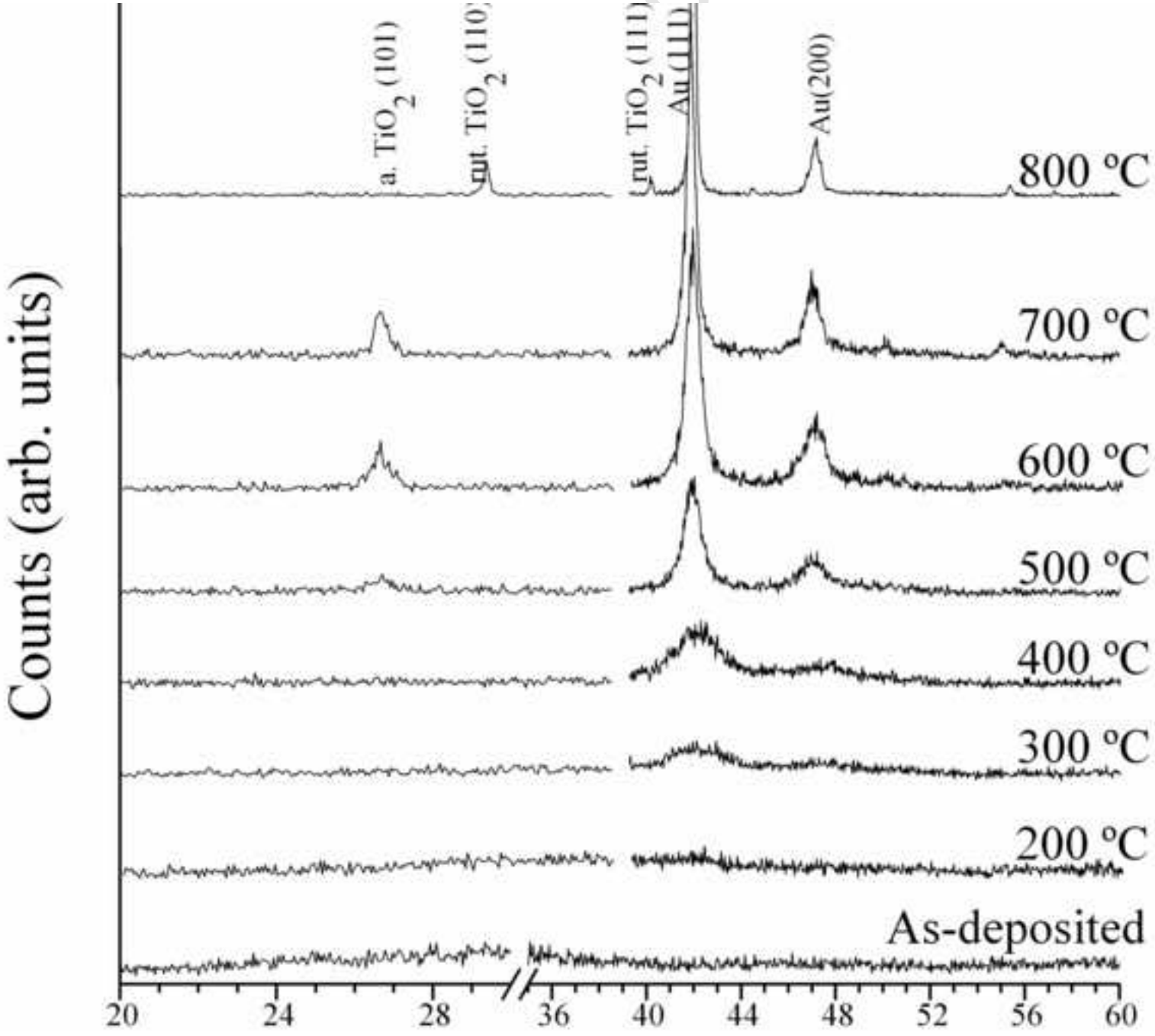

Fig. 3. Grain size obtained by integral-breadth analysis of Ti:O

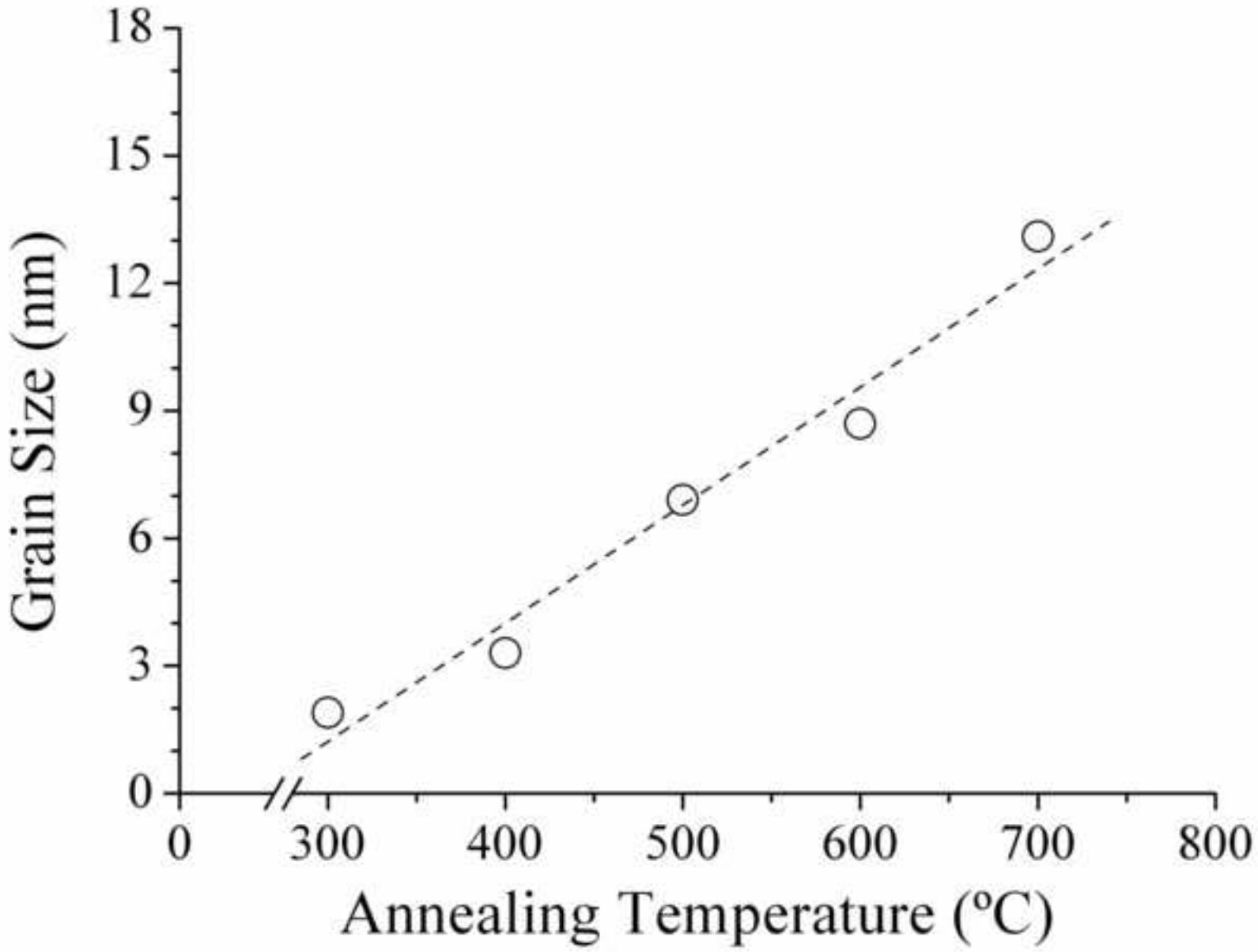

Fig. 4. Reflectivity as a function of the annealing temperature

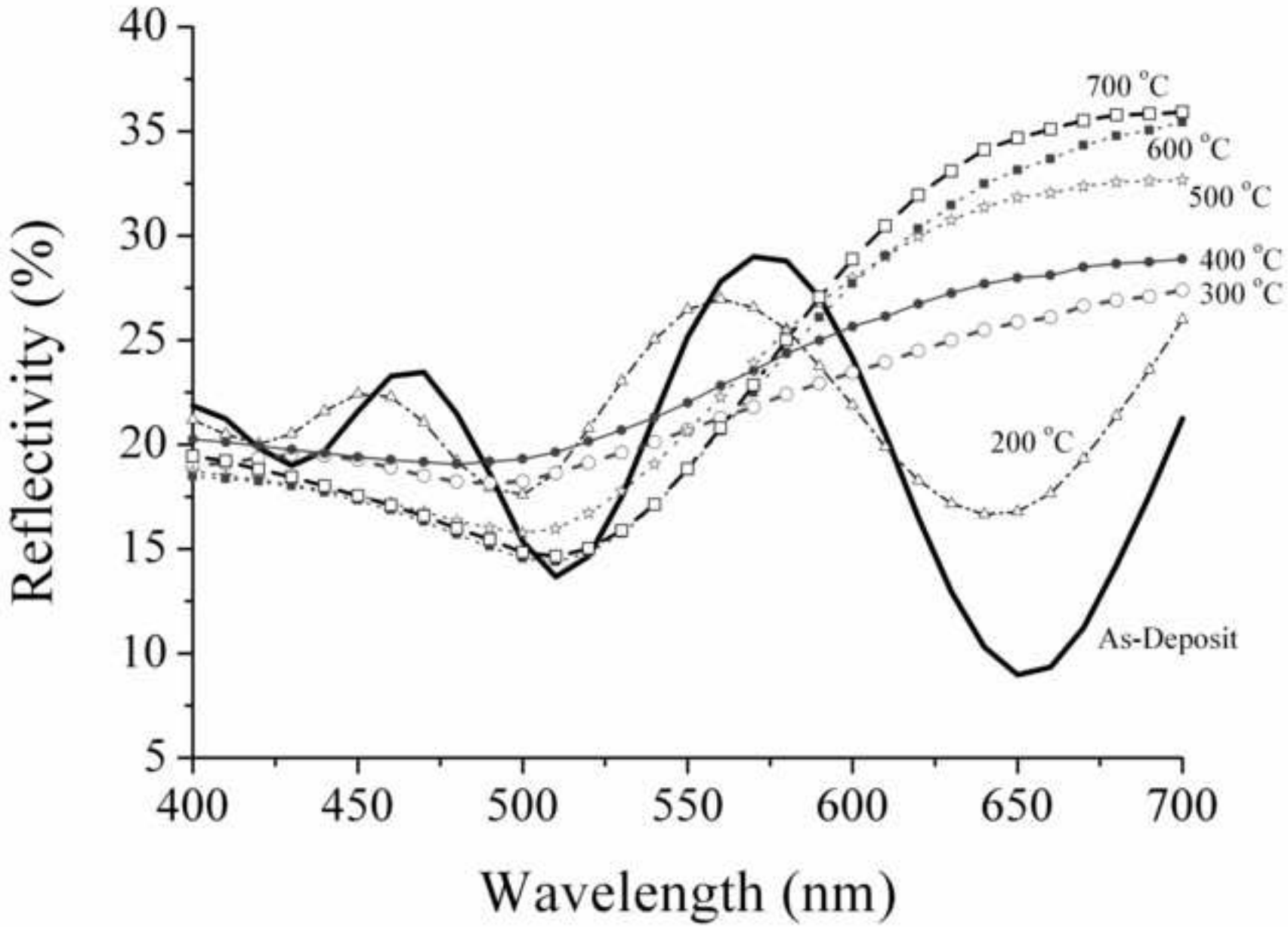

Fig. 5. CIELa*b* variation with the annealing temperature of Ti

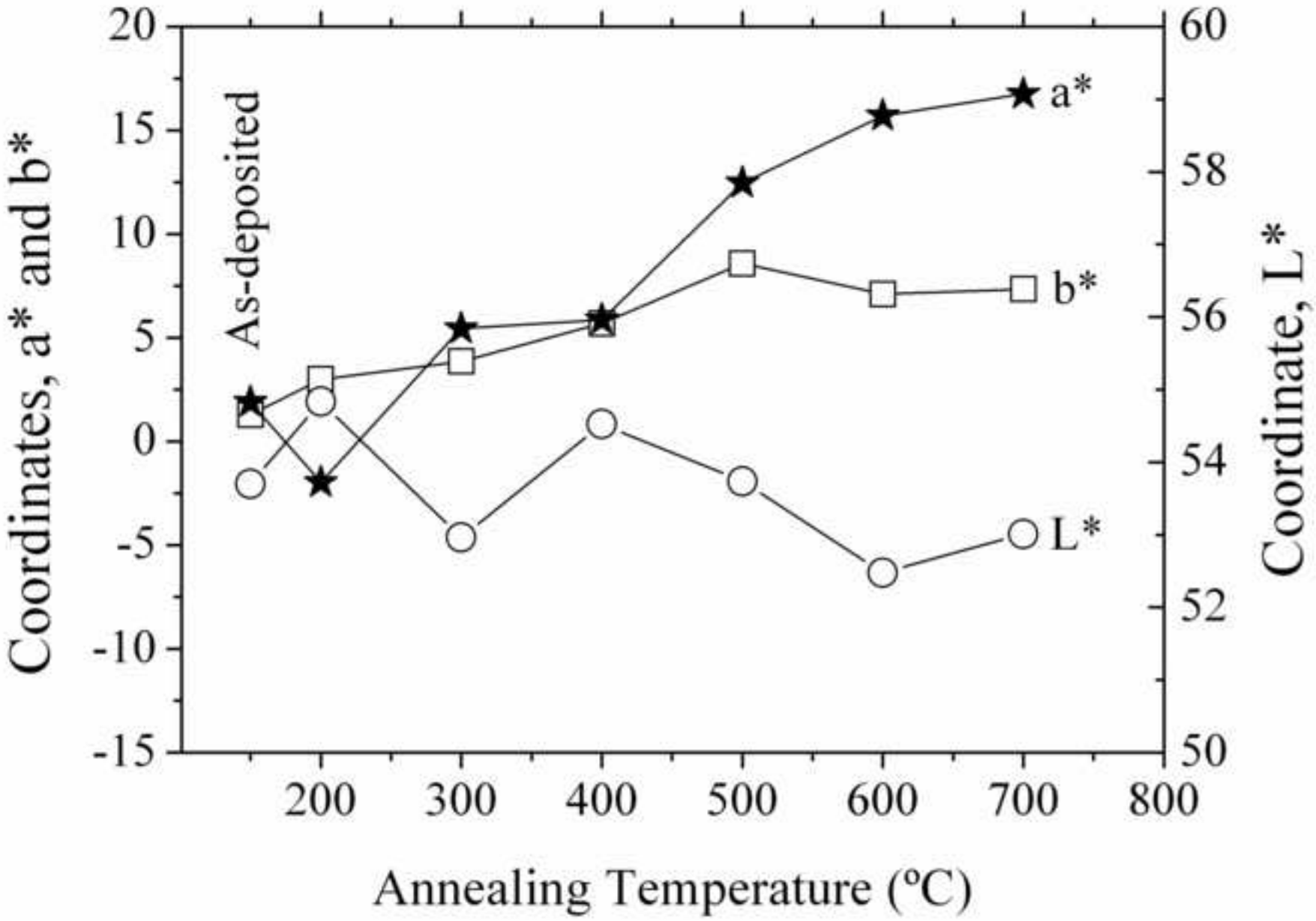

Fig. 5. CIELa*b* variation with the annealing temperature of Ti

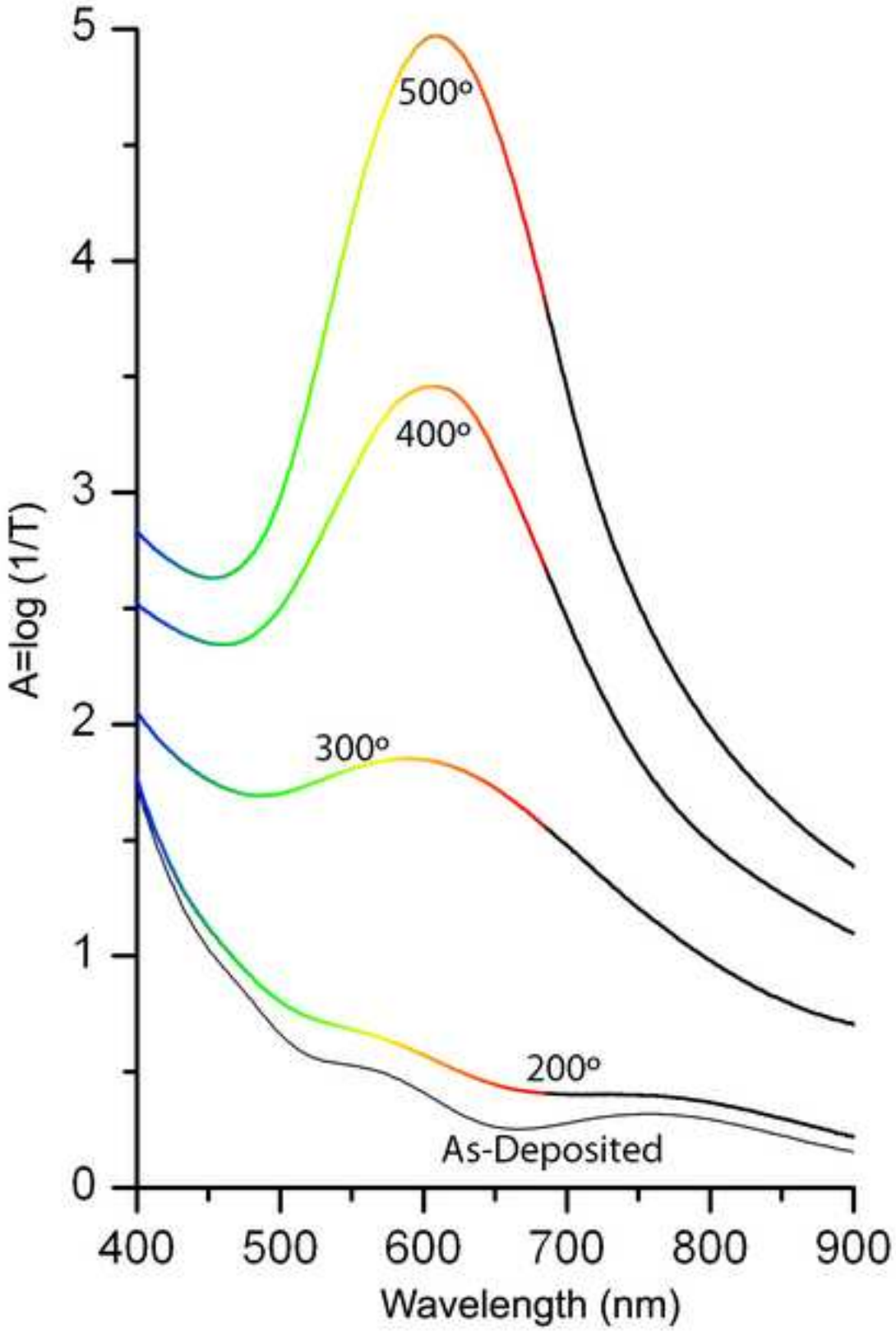

Fig. 7. a) Morphology of hertzian cracks during the track of scr

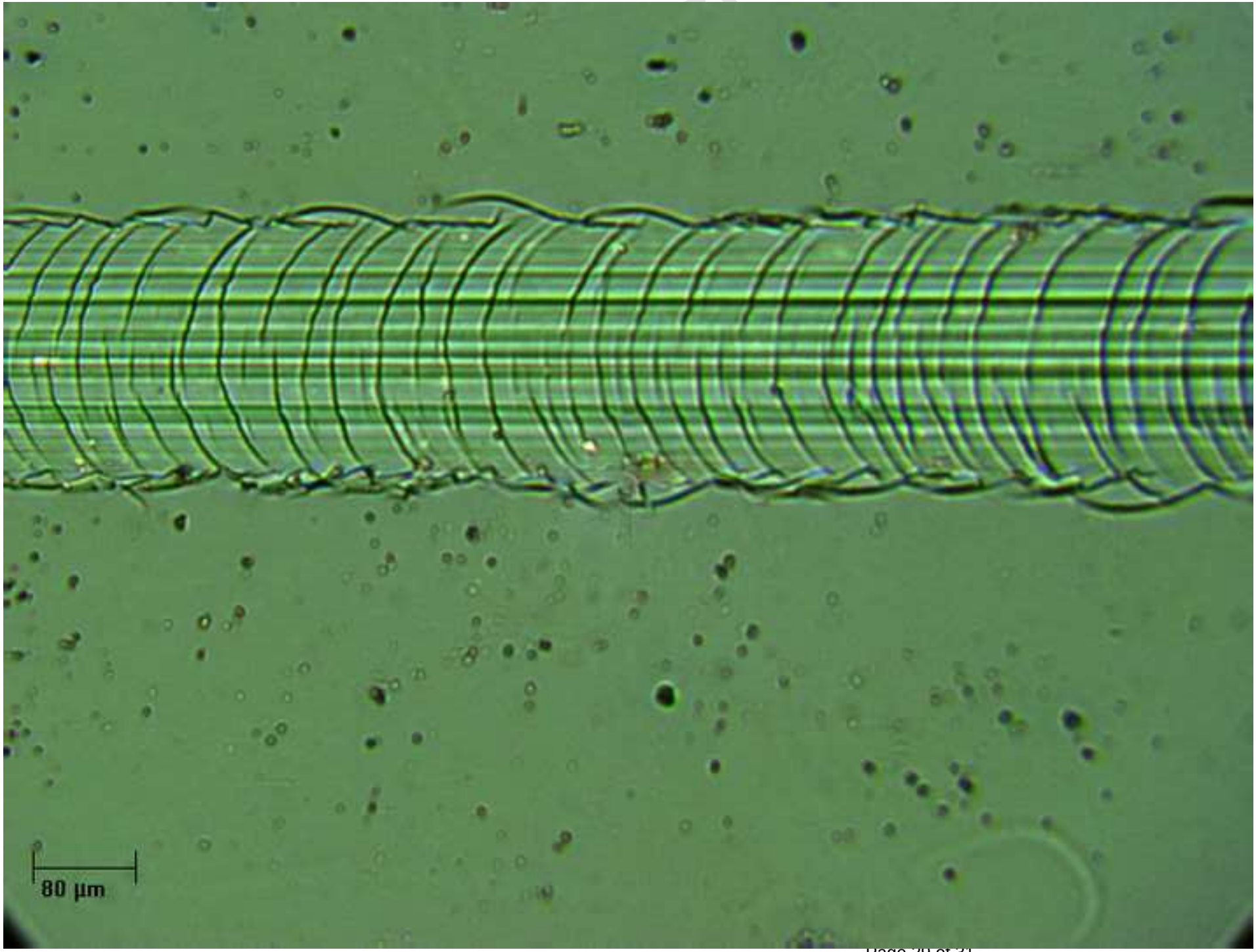

b) Final step of the scratch test where it can be seen that the

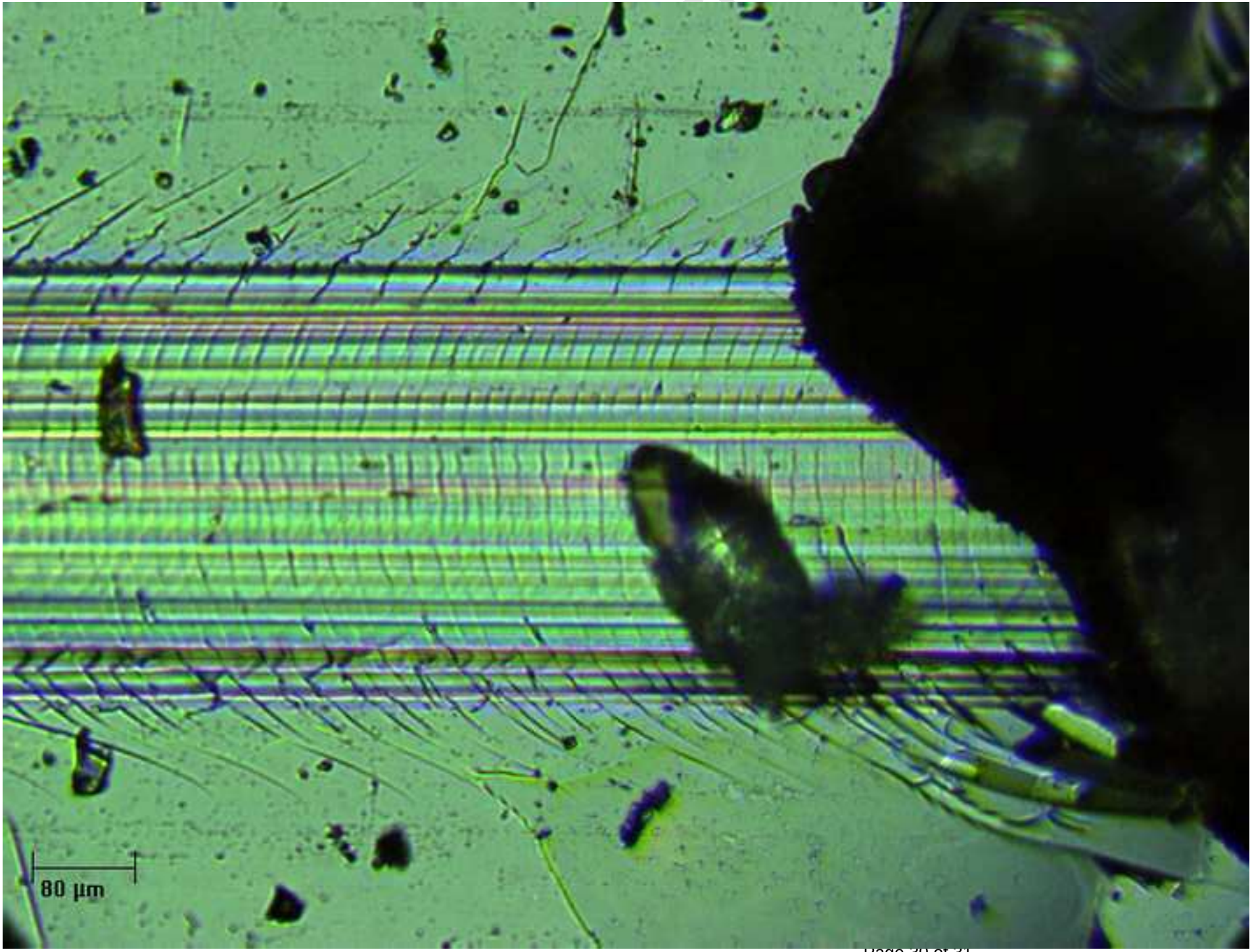

Table I. Mechanical properties values of TiO2:Au at different annealing temperatures.

	Nanoindentation test					Scratch test	
Annealing temperature	**Depth Max (nm)**	**Depth plastic (nm)**	**Load maximum (mN)**	**$HB_{0.8mN}$ (GPa)**	**E (GPa)**	**Li/ N**	**Lf/N**
As-deposited	62.3±1.3	51.8±1.7	0.83±0.01	5.9±0.3	136.8±9.0	7.1±1.1	73.5±0.8
400	68.1±2.2	58.3±2.5	0.83±0.01	5.0±0.3	135±13.4	7.3±1.6	48.8±1.3
500	60.5±1.1	49.2±1.7	0.83±0.01	6.4±0.3	131.9±10.8	7,8±1.3	43.5±2.1
600	55.4±1.8	44.7±1.9	0.83±0.01	7.5±0.5	149±12.9	5.6±1.2	45.9±1.4